

Cosmological Constraints on Long-Lived Particles Using Dimension-Six Effective Operators

Mickael V. S. de Farias^{1,2,*}, Rodrigo Holanda^{1,*}, Matheus M. A.

Paixão^{1,2,†}, Farinaldo S. Queiroz^{1,2,3,4,‡} and Priscila V. dos Santos^{2,5*}

¹*Departamento de Física, Universidade Federal do Rio Grande do Norte, 59078-970, Natal, RN, Brasil*

²*International Institute of Physics, Universidade Federal do Rio Grande do Norte, Campus Universitario, Lagoa Nova, Natal-RN 59078-970, Brazil*

³*Millennium Institute for Subatomic Physics at the High-Energy Frontier (SAPHIR) of ANID, Fernández Concha 700, Santiago, Chile*

⁴*Departamento de Física, Facultad de Ciencias, Universidad de La Serena, Avenida Cisternas 1200, La Serena, Chile and*

⁵*Universidade Federal de Pernambuco, Centro Acadêmico do Agreste*

Long-lived particles (LLPs) provide an interesting window into physics beyond the Standard Model, offering characteristic signatures at colliders and in cosmology. In this work, we investigate LLPs decays into dark matter. If the lifetime of LLPs are longer than 10^4 s, the decay products can disrupt the synthesis of light nuclei in the early universe and alter Big Bang Nucleosynthesis (BBN) predictions. If the LLP is much heavier than the dark matter particle, the decay contributes to the number of effective neutrino species, N_{eff} . We describe these decays via dimension-six effective operators and outline the parameter space in which such decays obey cosmological bounds stemming from BBN, structure formation, Cosmic Microwave Background, and Baryon Acoustic Oscillation data.

I. INTRODUCTION

Long-lived particles have gained increasing attention due to their interesting signatures at colliders and cosmological observables. However, the lifetime being tested at these laboratories are rather different. While colliders are sensitive to short-lived particles that decay within a few meters of the detector, cosmological probes test very long lived particles with a lifetime longer than a second. Theoretically speaking, very long-lived particles are amenable to a suppression mechanism involving their interactions with Standard Model (SM) particles to justify their long lifetime, conversely to SM particles, which are generally short-lived. This suppression mechanism either occurs in the coupling constant or in the energy scale that drives the interactions. If the natural scale that governs the interaction with the SM particle is very large, say the Planck Scale, the lifetime of the decaying particle is large, as happens in some supersymmetric models, where the neutralino decays into a gravitino plus a photon [1]. The implication of long-lived particles in cosmology has been considered in several studies [2–7].

A particular, we will explore the implication of LLP decays to the effective number of relativistic species, N_{eff} using an effective field theory (EFT) approach, which captures new physics effects for energies much lower the cut-off scale, Λ [8, 9]. These operators are suppressed by inverse powers of Λ that govern the decay and, consequently, the cosmological observables. We will assume that such LLPs are embedded in a dark sector with a stable dark matter candidate. Therefore, it is reasonable to assume these dark states come in pairs and for this reason, dimension-six effective operators describe more realistic interactions. For instance, the LLP may decay into the lightest odd particle (dark matter) plus a lepton, photon, or quark or even decay into unstable dark states that later

decay into Standard Model particles [1, 10–13]. As far as Big Bang Nucleosynthesis (BBN) and the Cosmic Microwave Background (CMB) are concerned, final state electrons and photons will induce similar effects. Accounting for hadronic decays is highly non-trivial due to the complexity of dealing with hadronic processes at low energies [14–23].

Thus, for concreteness, we will analyze decays of the type $X_1 \rightarrow X_2 + \gamma$, where X_1 is the LLP and X_2 is the lightest odd particle, i.e. a dark matter particle that accounts for the overall dark matter density. As dark matter does not interact with photons directly, it is natural to expect a suppression via higher dimension operators (larger than five). In the regime $m_{X_1} \gg m_{X_2}$, we will show that this decay contributes to a raise in N_{eff} . In other words, LLP decays can be a source of an extra radiation component in the early universe [24–28], and consequently alleviate the Hubble tension [29, 30]. The interesting aspect of this mechanism is the presence of the photon that provides a visible signature of this decay process, contributing to the diffuse photon background and serving as an indirect probe of the dark sector.

One could invoke dimension five effective operators, but they lead to relatively large decay widths and dangerously small lifetimes, requiring an energy scale larger than the Planck scale to reconcile with cosmological bounds [31]. We show that dimension-six operators relax this conclusion and, interestingly, allow weak-scale dark matter for energy scales much below 10^{15} GeV. That said, we consider two cases: (i) fermion dark matter and (ii) vector dark matter. Later we derive the corresponding decay width, and the relevant cosmological constraints [32–38]. We will observe that there is a rich interplay between particle physics and cosmology, particularly with N_{eff} ¹.

The paper is structured as follows: *section II* introduces the LLP decays into dark matter; *section III* discusses the im-

*

† matheus.mapaixao@gmail.com

‡ farinaldo.queiroz@ufrn.br

¹ We would like to dedicate this work to the memory of Raimundo Silva, who was a great collaborator and helped to build a bridge between particle physics and cosmology at UFRN.

plications for the Hubble constant; *section IV* addresses the relevant bounds; *section V* describes the effective field theory approach and outlines the viable parameter space before conclusions in *section VI*.

II. LLP DECAYS AND N_{eff}

In contexts where the scale of the new physics is unknown or inaccessible directly in particle accelerators, the EFT approach is particularly useful [39]. An EFT can be constructed by specifying three fundamental ingredients: its degrees of freedom (which may or may not be imposed by symmetries); the symmetries that constrain the system's dynamics, reflecting the effective action; and the expansion parameter. From this formalism, effects of new physics and possibly heavy-states of the dark sector can be incorporated through the inclusion of higher-dimensional effective operators that connect the visible and dark sectors.

At early times the energy density of radiation in Universe described by Λ CDM model is composed mostly by radiation, with photon and neutrinos being the dominant relativistic species at the time, i.e., $\rho_{\text{rad}} = \rho_\gamma + \rho_{1\nu}N_\nu$, in which ρ_γ represents the energy density of the photons, while $\rho_{1\nu}$ denotes the energy density of a single standard model neutrino species, where N_ν stands for neutrino species number.

Therefore, the energy density is the sum of background photons and neutrinos [40, 41] and any extra component, beyond the Λ CDM as,

$$\rho_{\text{rad}} = \rho_\gamma + N_\nu \rho_{1\nu} + \rho_{\text{extra}}. \quad (1)$$

This extra source of radiation is known in the literature as dark radiation. We can write this dark radiation in terms of the radiation caused by one neutrino species [42],

$$\rho_{\text{extra}} = \rho_{1\nu} \Delta N_{eff}, \quad (2)$$

where N_{eff} is the effective number of relativistic species. $\Delta N_{eff} = N_{eff} - N_\nu$. This term *effective* is appropriate because N_{eff} is not an integer number. In the Λ CDM, N_{eff} is sensitive to the time of neutrino decoupling, thus it has a temperature dependence. That said, the total radiation is found to be,

$$\rho_{\text{rad}} = \rho_\gamma + N_{eff} \rho_{1\nu}. \quad (3)$$

Studies related to the Cosmic Microwave Background constrain N_{eff} in terms of the cosmological parameters such as the Hubble constant [43, 44]. Adopting the matter-radiation equality as a reference for the computation of ΔN_{eff} , from Eq. (2) we can define,

$$\Delta N_{\text{eff}} = \frac{\rho_{\text{extra}}(t_{\text{eq}})}{\rho_{1\nu}(t_{\text{eq}})}. \quad (4)$$

In summary, a positive contribution to N_{eff} will automatically increase ρ_{rad} and, as a result, the Hubble constant [41] extracted from CMB measurements. In more general terms,

N_{eff} does not represent a neutrino species. It reflects the number of relativistic degrees of freedom at a given temperature. In the scenario considered here, the contribution to N_{eff} arises from a relativistic population of the particle X_2 produced from the decay of the LLP. As the universe expands, the energy of the X_2 particles are redshifted and diminished over time, up to the point of contributing to N_{eff} until the epoch of matter-radiation equality, mimicking the effect of an extra neutrino species and thereby alleviating the Hubble tension [45].

We describe below how this LLP decay can contribute to N_{eff} . In the rest frame of the LLP particle, the four-momenta of the particles read,

$$\begin{aligned} p_{X_1} &= (m_{X_1}, \mathbf{0}), \\ p_{X_2} &= (E_{X_2}(\mathbf{p}), \mathbf{p}), \\ p_\gamma &= (|\mathbf{p}|, -\mathbf{p}), \end{aligned} \quad (5)$$

where E_{X_2} and \mathbf{p} stand for the energy and the trimomentum associated with the dark matter particle X_2 , respectively. Immediately after the decay, the four-momenta conservation gives us,

$$|p_{X_2}(\tau)| = |\mathbf{p}| = \frac{1}{2} m_{X_1} \left[1 - \left(\frac{m_{X_2}}{m_{X_1}} \right)^2 \right], \quad (6)$$

$$E_{X_2}(\tau) = m_{X_2} \left(\frac{m_{X_1}}{2m_{X_2}} + \frac{m_{X_2}}{2m_{X_1}} \right), \quad (7)$$

in which τ is the lifetime of the LLP, X_1 . In the case where $m_{X_1} \gg m_{X_2}$, the initial energy will be equally distributed between the photon and the dark matter, with both contributing to the radiation content. In addition, it is useful to define the Lorentz factor,

$$\gamma_{X_2}(\tau) = \frac{m_{X_1}}{2m_{X_2}} + \frac{m_{X_2}}{2m_{X_1}}, \quad (8)$$

in such manner that $E_{X_2}(\tau) = m_{X_2} \gamma_{X_2}(\tau)$.

The expansion of the universe redshifts the momentum of the particle, becoming inversely proportional to the scale factor $\mathbf{p}_{X_2}^2 \propto 1/a^2$ [46]. As a consequence,

$$\begin{aligned} E_{X_2}^2 - m_{X_2}^2 &= \mathbf{p}_{X_2}^2 \propto \frac{1}{a^2} \\ \Rightarrow (E_{X_2}^2(t) - m_{X_2}^2) a^2(t) &= (E_{X_2}^2(\tau) - m_{X_2}^2) a^2(\tau) \\ \Rightarrow E_{X_2}(t) &= m_{X_2} \left[1 + \left(\frac{a(\tau)}{a(t)} \right)^2 (\gamma_{X_2}^2(\tau) - 1) \right]^{1/2}. \end{aligned} \quad (9)$$

Computing the ratio $a(\tau)/a(t)$ in the last equality and adopting Eq. (8), we can define a Lorentz factor $\gamma_{X_2}(t)$ as,

$$\gamma_{X_2}(t) = \left\{ 1 + \frac{(m_{X_1}^2 - m_{X_2}^2)^2}{4m_{X_2}^2 m_{X_1}^2} \left(\frac{\tau}{t} \right) \right\}^{1/2}, \quad (10)$$

which is the boost factor acquired by X_2 due the decay of the LLP. In the limit $m_{X_1} \gg m_{X_2}$ it reduces to,

$$\gamma_{X_2}(t_{\text{eq}}) - 1 \approx \frac{m_{X_1}}{2m_{X_2}} \sqrt{\frac{\tau}{t_{\text{eq}}}}. \quad (11)$$

The total energy of the dark matter particles ought to include those produced from the LLP decay so that [47, 48],

$$E_{\text{DM}} = N_{\text{HDM}} m_{X_2} (\gamma_{X_2} - 1) + N_{\text{CDM}} m_{X_2}, \quad (12)$$

where N_{HDM} is the number of dark matter particles produced via the LLP decay. N_{CDM} accounts for the number of dark matter particles produced via a thermal mechanism. The ratio between the energy densities of the two aforementioned components is given by,

$$\frac{\rho_{\text{HDM}}}{\rho_{\text{CDM}}} = \frac{n_{\text{HDM}} m_{X_2} (\gamma_{X_2} - 1)}{n_{\text{CDM}} m_{X_2}} \equiv f (\gamma_{X_2} - 1), \quad (13)$$

where n_{HDM} and n_{CDM} are the number densities and f the ratio between these two quantities. In other words, f determines the fraction of dark matter particles produced via the LLP decay.

Therefore, using Eq. (13) together with the definition of ΔN_{eff} in Eq. (4), we obtain that the extra relativistic degrees of freedom, given by this formalism, can be computed as,

$$\Delta N_{\text{eff}} = \frac{\rho_{\text{CDM}} f (\gamma_{X_2} - 1)}{\rho_{1\nu}}. \quad (14)$$

At matter-radiation equality, the ratio between the energy density of cold dark matter and that of one neutrino is $\rho_{1\nu}/\rho_{\text{CDM}} = 0.16$, which precisely mimics the effect of one neutrino species in the Hubble rate at later times [24]. Using this information and Eq.(14) we find,

$$\Delta N_{\text{eff}} = \frac{f (\gamma_{X_2} - 1)}{0.16}. \quad (15)$$

Substituting Eq.(11) into Eq.(15) we get,

$$\Delta N_{\text{eff}} \approx 2.5 \times 10^{-3} \sqrt{\frac{\tau}{10^6 \text{s}}} \times f \frac{m_{X_1}}{m_{X_2}}, \quad (16)$$

Therefore, particle physics and cosmology are intertwined. A particle physics process has a direct impact on N_{eff} and consequently on the Hubble constant extracted from CMB measurements. Our goal in this work is set limits on LLP decays to dark matter.

III. CONSTRAINTS

A. CMB and BAO Surveys

Many works have explored the positive correlation between N_{eff} and H_0 to solve the H_0 problem. Estimates of the Hubble constant H_0 inferred from early-Universe observations such as those stemming from the Cosmic Microwave Background [49] are systematically lower than those obtained from independent low-redshift probes [50–54]. This growing mismatch, now supported by multiple observational techniques, suggests a possible limitation of the standard cosmological model rather than a mere statistical fluctuation

[55, 56]. In particular, a study using Cepheid Observations from the James Webb Telescope obtained $H_0 = (73.49 \pm 0.93) \text{ km s}^{-1} \text{ Mpc}^{-1}$ [57]. A community report found $H_0 = 73.50 \pm 0.81 \text{ km s}^{-1} \text{ Mpc}^{-1}$ [58], which translates into a 7.1 σ discrepancy.

It is known that the Hubble rate at the last-scattering surface can be parametrized as [59],

$$H_{ls} = 100 \text{ km s}^{-1} \text{ Mpc}^{-1} \omega_r^{1/2} (1 + z_{ls}) \sqrt{1 + \frac{w_m}{w_r} \frac{1}{1 + z_{ls}}} \quad (17)$$

where $z_{ls} = 1080$, $\omega_m = \Omega_m h^2$, and

$$w_r = \left[1 + \frac{7}{8} N_{\text{eff}} \left(\frac{4}{11} \right)^{4/3} \right] w_\gamma \quad (18)$$

with $w_\gamma = 2.45 \times 10^{-5}$.

Hence, it is clear that the H_0 value inferred from CMB is indeed positively correlated with N_{eff} . However, one cannot arbitrarily increase N_{eff} simply focusing on its impact on H_0 . An increase in N_{eff} can also significantly impact the sound horizon which disagrees with BAO measurements. Therefore, having a large $N_{\text{eff}} > 0.3$ as solution to H_0 is deemed implausible [60]. Moreover, BAO measurements depend on the sound horizon at the drag epoch, which is the distance that sound can travel between the Big Bang and the drag epoch. It quantifies the time when the baryons decoupled from photons. A combination of BAO and CMB data imposed $N_{\text{eff}} = 3.1 \pm 0.17$ [61]. A recent study of BBN data taking into account dark radiation has imposed looser bound, namely $\Delta N_{\text{eff}} < 0.74$ at 95% C.L. [62]. In this range, N_{eff} can still help alleviate the Hubble tension [63], but not solve it. Apparently, the H_0 problem requires much more complex solutions than a simple connection to N_{eff} [60, 63]. That said, for our reasoning, we will impose the CMB-BAO limit $\Delta N_{\text{eff}} < 0.3$ [61] from now on. The precise value will not change our qualitative conclusions, as we describe below.

B. BBN constraints

Big Bang nucleosynthesis (BBN) constitutes a cornerstone of early-universe cosmology, and its successful agreement with light-element abundances tightly constrains any late injection of energy around the BBN epoch. In particular, the decay channel $X_1 \rightarrow X_2 + \gamma$ can trigger electromagnetic cascades [1, 6]. This extra electromagnetic component may modify the primordial abundances of light nuclei such as helium and deuterium. Before presenting our final constraints, we briefly summarize how these bounds are obtained. Prior to the decay of X_1 , the universe already contains a thermal photon background; after the decay, the photons observed in the CMB comprise both of this original background and the contribution from the decay-induced cascade. Accordingly, we express the mean CMB photon energy as,

$$E_\gamma^{\text{CMB}} = E_\gamma^{\text{BG}} \left(\frac{n_\gamma^{\text{BG}}}{n_\gamma^{\text{CMB}}} \right) + E_\gamma \left(\frac{n_\gamma}{n_\gamma^{\text{CMB}}} \right), \quad (19)$$

where E_γ^{BG} denotes the mean energy of the background photons, E_γ is the mean energy of the photons produced in the decay, n_γ^{BG} is the background photon number density, n_γ^{CMB} is the total CMB photon number density, and n_γ represents the number density of photons generated in our scenario. Knowing that the decay $X_1 \rightarrow X_2 + \gamma$ implies that $n_{X_1} = n_{X_2} = n_\gamma$, where n_γ is the number density of photons added to the universe due to the decay, we obtain the overall electromagnetic energy injected by the LLP,

$$\zeta_{EM} \equiv E_\gamma Y_\gamma = E_\gamma Y_{X_1}, \quad (20)$$

where $Y_\gamma = n_\gamma/n_\gamma^{CMB}$, and $Y_{X_1} = n_{CDM} \times f/n_\gamma^{CMB}$.

Eq. (20) quantifies the electromagnetic energy injected by the decay. Using the definition of critical density ($\rho_c \equiv 3H/(8\pi G)$), the definition of density parameter ($\Omega \equiv \rho/\rho_c$), the cold particle energy density ($\rho = nm$), and the time evolution of number density of CMB photons ($n_\gamma^{CMB} = n_{\gamma,0}^{CMB}/a^3$) [64], we can rewrite Y_{X_1} as,

$$Y_{X_1} = \frac{f}{m_{X_1} n_{\gamma,0}^{CMB}} \times \Omega_{CDM,0} \rho_{c,0}, \quad (21)$$

where $\Omega_{CDM} a^3 \rho_c = \Omega_{CDM,0} \rho_{c,0}$ [64].

Plugging in the known quantities, $\rho_{c,0} \simeq 1.05 \times 10^{-5} h^2 \text{GeV}/\text{cm}^3$, $n_{\gamma,0}^{CMB} = 411 \text{cm}^{-3}$ and $\Omega_{CDM,0} h^2 = 0.12$ we find,

$$Y_{X_1} = 3.01 \times 10^{-9} \left(\frac{\text{GeV}}{m_{X_1}} \right) \times f. \quad (22)$$

Assuming, $m_{X_1} \gg m_{X_2}$, the injected energy into the plasma per decay is $E_\gamma = m_{X_1}/2$. Consequently, the electromagnetic radiation is given by,

$$\zeta_{EM} = E_\gamma Y_{X_1} = 1.5 \times 10^{-9} \text{GeV} \times \left(f \frac{m_{X_1}}{m_{X_2}} \right). \quad (23)$$

Thus, the total electromagnetic energy injected into the process, as determined by Eq.(20), is tied to the properties of the dark sector. Therefore, we can constrain the properties of the dark sector using BBN observations.

In Figure 1 we exhibit the BBN limits in terms of the ratio $f m_{X_1}/m_{X_2}$ and the lifetime of the decay, assuming prompt decay. The shaded regions correspond to parameter space ruled out due to the over-destruction of helium-4, lithium-7, and deuterium, or trigger nuclear reactions that overproduce deuterium in conflict with astronomical abundance measurements [19, 20, 65–69]. At very early times (before 10^4s) injected photon thermalize with background photons doing no harm to the abundances of light elements. At later times, thermalization becomes inefficient, and for this reason, the constraints become stronger with the lifetime. The green region represents the parameter space that produces $\Delta N_{eff} = 0.1 - 0.3$.

C. Spectral Distortions

The injection of electromagnetic energy may also distort the frequency dependence of the CMB spectrum. Double

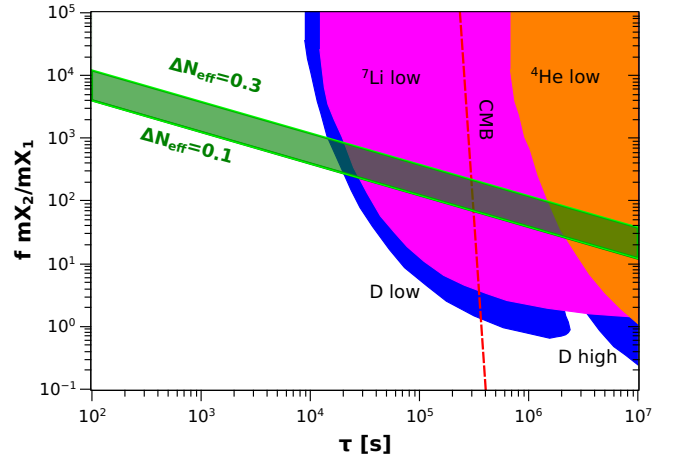


Figure 1. BBN bounds based on light element abundances and CMB constraint stemming from spectral distortion of the CMB. See text for details. The green region delimits the parameter space that yields $\Delta N_{eff} = 0.1 - 0.3$. Using the positive correlation between ΔN_{eff} and H_0 one could raise H_0 and alleviate the Hubble tension.

Compton scattering ($\gamma e^- \rightarrow \gamma \gamma e^-$), and bremsstrahlung ($e^- X \rightarrow e^- X \gamma$) are not very efficient for $\tau > 10^4 \text{s}$. As a result the CMB spectrum relaxes to a Bose-Einstein distribution function with a chemical potential different from zero with,

$$\mu = 8 \times 10^{-4} \left(\frac{\tau^4}{10^6 \text{s}} \right)^{1/2} \left(\frac{\zeta_{EM}}{10^{-9} \text{GeV}} \right) e^{(-\tau_{dc}/t)^{5/4}}, \quad (24)$$

where τ_{dc} is a constant that depends on the baryonic density[1]. Using Eq.(23) we can plot the CMB bound in the plane $f m_{X_1}/m_{X_2} \times \tau$ as shown in Figure 1. In the region of interest, the CMB limit is less competitive than the BBN one.

D. Structure Formation

The median velocity of the decay product at a given time t for the two-body decay is,

$$v_{1,2,\text{med}}(t) \sim \frac{a_{\text{dec}}/a(t)p}{\sqrt{(a_{\text{dec}}/a(t)p)^2 + m_{1,2}^2}}. \quad (25)$$

The important quantity regarding structure formation is the free-streaming distance, which can be written as,

$$k_{\text{fs}}(a) = \frac{\sqrt{\rho a^2/2M_{\text{P}}^2}}{v_{\text{med}}(a)} = \sqrt{\frac{3}{2}} \frac{aH(a)}{v_{\text{med}}(a)}, \quad (26)$$

where for $k > k_{\text{fs}}$, the growth of structure is suppressed. Hot dark matter (HDM) particles have large free-streaming. The abundance of hot dark matter is often quoted in terms of the massive neutrinos abundance [70, 71]. The best cosmological probe of constraining massive neutrinos acting as HDM is the galaxy power spectrum. The latest result from the DESI

collaboration imposes the sum of the neutrino masses to be $\Sigma m_\nu < 0.113$ eV [61], which translates into $\Omega_\nu h^2 < 0.001$, and consequently $f = \Omega_{HDM}/\Omega_{CDM} < 0.009$. Roughly speaking, a mechanism that produces a population of HDM is limited to account for at most 0.9% of the overall dark matter abundance. For this reason, we will set $f = 0.009$ hereafter.

E. Entropy Injection

In the radiation-dominated era the difference in entropy between two initial times, before the decay, and a final time, after the decay, is found to be,

$$\frac{S_f}{S_i} = \frac{g_{*s}^f T_f a_f^3}{g_{*s}^i T_i a_i^3}, \quad (27)$$

where T is the photon temperature, while g_{*s} is defined in terms of the bosonic (g_b) and fermion (g_f) degrees of freedom as. As the temperature is related to the photon density, which in turn depends on g_* , after the LLP decay, the change in entropy ratio becomes [72],

$$\frac{S_f - S_i}{S_i} = \frac{\Delta S}{S_i} = \frac{g_{*s}^f}{g_{*s}^i} \left(\frac{g_*^i}{g_*^f} \right)^{3/4} - 1 \simeq 0.05 \Delta N_{eff}. \quad (28)$$

Having in mind the existing limits on ΔN_{eff} , we conclude that the change in entropy is small, in agreement with CMB observations and BBN.

IV. DIMENSION-6 EFFECTIVE LAGRANGIANS

The results developed so far are quite general and model-independent, applying to all effective Lagrangians that describe a LLP decaying into relativistic DM and a photon. The specific details of the model arise when computing the decay width and inserting it into Eq. (16) in the form of the lifetime. In this sense, it is possible to obtain a relation between the cutoff energy scale Λ , the extra effective number of neutrino species ΔN_{eff} , and the masses of the particles involved in the decay. We do this exercise for: a) fermion dark matter and b) for vector dark matter.

Case A: Fermion Dark Matter A fermion LLP may decay into a fermion dark matter particle and a photon via the Lagrangian

$$\mathcal{L}_{eff} = \frac{1}{\Lambda^2} \{ i \bar{X}_1 \gamma^\mu \partial^\nu X_2 F_{\mu\nu} + \text{h.c.} \}, \quad (29)$$

as illustrated in Figure 2.

We remind that X_1 and X_2 represent the LLP and dark matter field, respectively, and $F^{\mu\nu}$ the electromagnetic field strength. This dimension-6 operator couples the fermion bilinear $\bar{X}_1 \gamma^\mu \partial^\nu X_2$ to $F_{\mu\nu}$, giving rise to the two-body decay

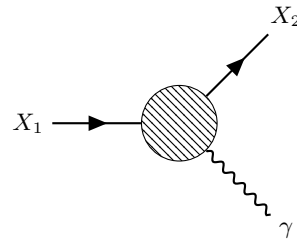


Figure 2. Diagrammatic representation of the decay $X_1 \rightarrow X_2 + \gamma$. In order to have relativistic production of dark matter, it is assumed that $m_{X_1} \gg m_{X_2}$.

$X_1 \rightarrow X_2 + \gamma$. After the LLP decay, the kick transferred to the dark matter particle will contribute to ΔN_{eff} as discussed in Section II. A straightforward computation of the decay width from Lagrangian Eq.(29) gives,

$$\Gamma = \frac{m_{X_1}^5}{32\pi\Lambda^4} \left[1 - \left(\frac{m_{X_2}}{m_{X_1}} \right)^2 \right]^3 \left[1 - \left(\frac{m_{X_2}}{m_{X_1}} \right) \right]^2 \approx \frac{m_{X_1}^5}{32\pi\Lambda^4}. \quad (30)$$

Inserting this relation into Eq. (16), we relate the LLP and dark matter masses for a fixed cutoff scale. Accordingly,

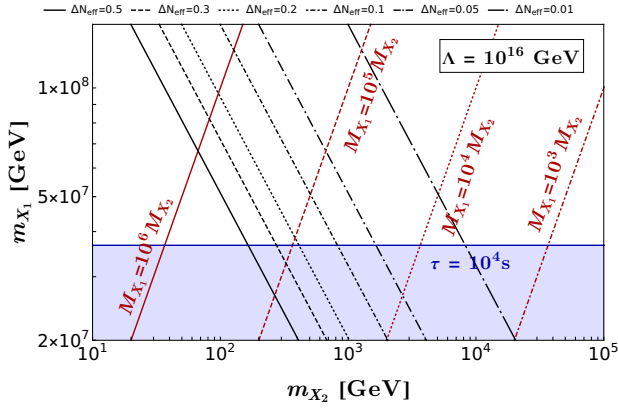
$$m_{X_1} = \left(\frac{32\pi\Lambda^4}{d m_{X_2}^2} \right)^{1/3}, \quad (31)$$

with d being an auxiliary constant depending on ΔN_{eff} as follows,

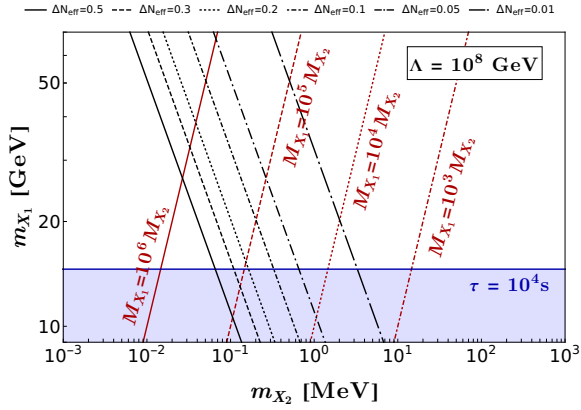
$$d = \frac{\Delta N_{eff}^2 \times 10^{12} \text{ s}}{25 f^2 \hbar (\text{GeV} \cdot \text{s})}. \quad (32)$$

Using Eq.(31) and Eq.(32) we relate the relevant quantities Λ , m_{X_1} and m_{X_2} to ΔN_{eff} .

We learned from Figure 1 that a lifetime longer than 10^4 s is excluded by BBN, having in mind the desired $f m_{X_2}/m_{X_1}$ ratio to yield $\Delta N_{eff} = 0.1 - 0.3$. Lower values of ΔN_{eff} can be obtained by decreasing the $f m_{X_2}/m_{X_1}$ ratio. In Figure 3(a) we delimit the parameter space that yields a lifetime $\tau \leq 10^4$ s and $\Delta N_{eff} = 0.01 - 0.5$ for $\Lambda = 10^{16}$ GeV. We repeated this exercise for $\Lambda = 10^8$ GeV in Figure 3(b). We remind the reader that we have assumed $f = 0.009$ throughout, as discussed previously.



(a)



(b)

Figure 3. Parameter space for the decay (29). Allowed regions in the long-lived particle (m_{X_1}) and dark matter (m_{X_2}) parameter space for different values of the energy scale Λ . The colored shaded area represents the BBN constraints $\tau \leq 10^4$ s [42]. The red lines indicate different values of the mother-to-daughter mass ratio.

In Figure 3(a), we cover dark matter masses going from 10 GeV up to 10^5 GeV. The shaded region is excluded by BBN. That said, we conclude that a large region of parameter space is free from cosmological bounds, but only a small one can contribute to $\Delta N_{eff} = 0.1 - 0.3$ and potentially raise the H_0 value. Interestingly, imposing $\Delta N_{eff} < 0.1$, we can set a lower mass limit on the dark matter that yields, namely $m_{X_2} > 1$ TeV. Once we lower the effective energy scale down to $\Lambda = 10^8$ GeV, we allow lower masses, as shown in Figure 3(b). In Figure 3(b), dark matter masses should lie in the MeV region to induce a $\Delta N_{eff} < 0.1$. Having dark matter masses below the TeV scale is an advantage of using effective operators of higher dimension compared to dimension-five effective operators [73].

Case B: Vector Dark Matter

If dark matter is a vector field, its production via LLP decay (see Figure IV) can be described by the Lagrangian form,

$$\mathcal{L}_{eff} = \frac{1}{\Lambda^2} G^\mu{}_\nu X^{\nu\alpha} F_{\mu\alpha}, \quad (33)$$

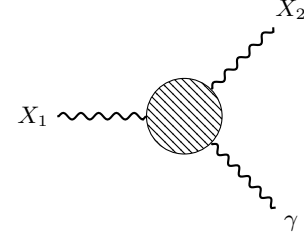


Figure 4. Diagram representing of the decay $X_1 \rightarrow X_2 + \gamma$ decay, where X_1 and X_2 are both vector fields.

From Eq.(33) we find the decay width,

$$\begin{aligned} \Gamma &= \frac{1}{96\pi\Lambda^4} \frac{m_{X_1}^7}{m_{X_2}^2} \left(1 - \frac{m_{X_2}^2}{m_{X_1}^2}\right)^3 \\ &\times \left[1 - 4 \left(\frac{m_{X_2}}{m_{X_1}}\right)^4 - \left(\frac{m_{X_2}}{m_{X_1}}\right)^6\right] \\ &\simeq \frac{m_{X_1}^7}{96\pi\Lambda^4 m_{X_2}^2}. \end{aligned} \quad (34)$$

Similarly to the preview process, we get a relation with respect to the energy scale as follows,

$$m_{X_1} = \left(\frac{96\pi\Lambda^4}{d}\right)^{1/5}, \quad (35)$$

where d is given in Eq.(32) with m_{X_1} not depending explicitly on m_{X_2} , implicating in straight lines in the m_{X_1} versus m_{X_2} plane. In Figure 5(a), we plot the region of parameter space in the $m_{X_1} - m_{X_2}$ plane which reproduces $\Delta N_{eff} > 0$ assuming $\Lambda = 10^{16}$ GeV.

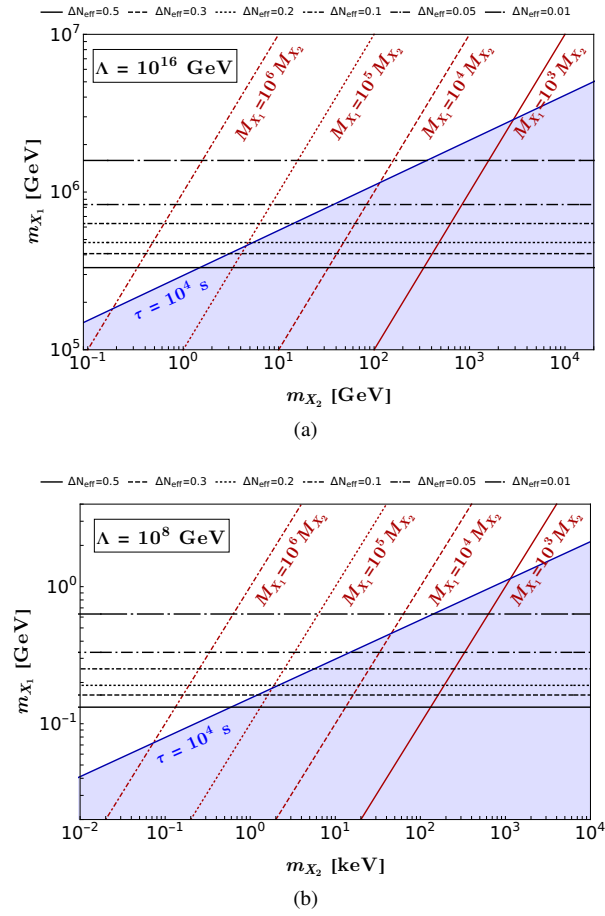


Figure 5. Parameter space for the decay (33). Again, The colored shaded area represents the BBN constrains $\tau \leq 10^4$ s, whereas the red lines delineates different values of the ratio m_{X_1}/m_{X_2} .

As aforementioned, the main distinction between the fermion dark matter and the vector dark matter is the relation between m_{X_1} and ΔN_{eff} ruled by Eq.(32). In Figure 5(a), we take $\Lambda = 10^{16}$ GeV. We conclude that the dark matter mass should be larger than ~ 10 GeV to induce $\Delta N_{eff} < 0.1$. Whereas for $\Lambda = 10^8$ GeV (see Figure 5(b)), only when $m_{X_2} > 10$ keV we can reproduce $\Delta N_{eff} < 0.1$. We highlight that, the entire parameter space with $\tau < 10^4$ s, which yields $\Delta N_{eff} < 0.3$ [61] is consistent with BBN, CMB and BAO data. There are clearly two ways clear outcomes: (i) once we enforce an upper limit on ΔN_{eff} , say $\Delta N_{eff} < 0.1$, we find a lower mass bound on the dark matter mass. The precise value depends on the dark matter nature and effective energy scale Λ ; (ii) if one wants to have LLP decays as a possible source of dark radiation to alleviate the tension between CMB and local measurements of H_0 an upper bound on the dark matter mass is found. Considering Figure 5(b) for concreteness, and imposing $0.1 < \Delta N_{eff} < 0.3$, we conclude that the dark matter mass should be smaller than 4 keV. Thus, observational cosmology can place constraints on the production mechanism of dark matter particles via its signatures on structures formation, BAO, BBN and particularly N_{eff} .

V. CONCLUSIONS

In this work, we investigate how effective dimension-6 operators can map the cosmological impacts of long-lived particles decays into dark matter. We investigated fermion and vector dark matter particles with mass m_{X_2} . Structure formation requires that only a fraction of the overall dark matter abundance should be produced via this mechanism. BBN imposes a lifetime shorter than 10^4 s to avoid conflict with observations of the primordial abundance of Deuterium and ^4He . A combination of BAO and CMB surveys impose $\Delta N_{eff} < 0.3$. That said, we computed the decay widths of the long-lived particles in terms of the relevant parameters and found a clear advantage of considering dimension-six effective operators in comparison with previous studies in the literature that were limited to dimension-five effective theories. Dark matter masses below the TeV scale have become viable. In particular, we found that ΔN_{eff} can constrain this dark matter production mechanism down to keV masses. Setting $\Lambda = 10^8$ GeV, sub-MeV fermion dark matter can yield $\Delta N_{eff} = 0.1 - 0.3$. The larger the dark matter mass, the smaller the effect on N_{eff} . Due to the properties of the interactions involved, LLPs decays into vector dark matter favor masses below the keV scale, whereas decays into fermion dark matter prefer masses below 1MeV, taking $\Lambda = 10^8$ GeV.

Two distinct outcomes emerge clearly from our analysis: (i) If we impose an upper bound on (ΔN_{eff}), for instance ($\Delta N_{eff} < 0.1$), we obtain a corresponding lower bound on the dark matter mass. The exact value of this bound depends on the nature of the dark matter candidate and on the effective energy scale (Λ); (ii) On the other hand, if long-lived particle (LLP) decays are invoked as a possible source of dark radiation with the intention of alleviating the tension between Cosmic Microwave Background measurements and local determinations of the Hubble constant (H_0), an upper bound on the dark matter mass arises. Our main results are summarized in Figures 3 and 5. In summary, cosmological observations going from structure formation, BBN, BAO to CMB are powerful probes for the production of dark matter resulted from LLPs decays.

VI. ACKNOWLEDGEMENTS

The authors thank Saulo Carneiro and Rafael Nunes for comments on the manuscript. RH acknowledges the support from CNPq through grant 308550/2023-4. MP acknowledges the support from CNPq through grant 151811/2024-5. MP also thanks the ICTP-Trieste and Mehrdad Mirbabayi for their hospitality while part of this work was carried out. MF was financed by the Coordenação de Aperfeiçoamento de Pessoal de Nível Superior - Brasil (CAPES) - Finance Code 001. FSQ acknowledges support from Simons Foundation (Award Number:1023171-RC), CNPq 403521/2024-6, 408295/2021-0, 403521/2024-6, 406919/2025-9, 351851/2025-9, the FAPESP Grants 2021/01089-1, 2023/01197-4, ICTP-SAIRF 2021/14335-0, and the ANID-Millennium Science Initiative Program ICN2019_044. PVS and FSQ were partially funded

by FINEP under project 213/2024 and was carried out in part

through the IIP cluster *bulletcluster*.

-
- [1] Jonathan L. Feng, Arvind Rajaraman, and Fumihiro Takayama. SuperWIMP dark matter signals from the early universe. *Phys. Rev. D*, 68:063504, 2003.
- [2] John R. Ellis, Dimitri V. Nanopoulos, and Subir Sarkar. The Cosmology of Decaying Gravitinos. *Nucl. Phys. B*, 259:175–188, 1985.
- [3] John R. Ellis, G. B. Gelmini, Jorge L. Lopez, Dimitri V. Nanopoulos, and Subir Sarkar. Astrophysical constraints on massive unstable neutral relic particles. *Nucl. Phys. B*, 373:399–437, 1992.
- [4] M. Kawasaki and T. Moroi. Electromagnetic cascade in the early universe and its application to the big bang nucleosynthesis. *Astrophys. J.*, 452:506, 1995.
- [5] T. Asaka, J. Hashiba, M. Kawasaki, and T. Yanagida. Spectrum of background x-rays from moduli dark matter. *Phys. Rev. D*, 58:023507, 1998.
- [6] Richard H. Cyburt, John R. Ellis, Brian D. Fields, and Keith A. Olive. Updated nucleosynthesis constraints on unstable relic particles. *Phys. Rev. D*, 67:103521, 2003.
- [7] Katarina Bleau, Joseph Bramante, and Christopher Cappiello. How effective is N_{eff} at discovering dark radiation in a cosmology with heavy particle decay? *JCAP*, 01:021, 2024.
- [8] Roberto Contino, Adam Falkowski, Florian Goertz, Christophe Grojean, and Francesco Riva. On the validity of the effective field theory approach to sm precision tests. *Journal of High Energy Physics*, 2016, 2016.
- [9] John Ellis, Verónica Sanz, and Tevong You. The effective standard model after lhc run i. *Journal of High Energy Physics*, 2015, 2015.
- [10] Jonathan L. Feng, Shu-fang Su, and Fumihiro Takayama. SuperWIMP gravitino dark matter from slepton and sneutrino decays. *Phys. Rev. D*, 70:063514, 2004.
- [11] Jose A. R. Cembranos, Jonathan L. Feng, Arvind Rajaraman, and Fumihiro Takayama. SuperWIMP solutions to small scale structure problems. *Phys. Rev. Lett.*, 95:181301, 2005.
- [12] Chris Kelso, C. A. de S. Pires, Stefano Profumo, Farinaldo S. Queiroz, and P. S. Rodrigues da Silva. A 331 WIMP Dark Radiation Model. *Eur. Phys. J. C*, 74(3):2797, 2014.
- [13] Mathias Garny and Jan Heisig. Interplay of super-WIMP and freeze-in production of dark matter. *Phys. Rev. D*, 98(9):095031, 2018.
- [14] John R. Ellis, Jihn E. Kim, and Dimitri V. Nanopoulos. Cosmological Gravitino Regeneration and Decay. *Phys. Lett. B*, 145:181–186, 1984.
- [15] J. Audouze, D. Lindley, and J. Silk. Big Bang Photosynthesis and Pregalactic Nucleon Synthesis of Light Elements. *Astrophys. J. Lett.*, 293:L53–L57, 1985.
- [16] Masahiro Kawasaki and Katsuhiko Sato. Decay of Gravitinos and Photodestruction of Light Elements. *Phys. Lett. B*, 189:23, 1987.
- [17] M. H. Reno and D. Seckel. Primordial Nucleosynthesis: The Effects of Injecting Hadrons. *Phys. Rev. D*, 37:3441, 1988.
- [18] Kazunori Kohri. Primordial nucleosynthesis and hadronic decay of a massive particle with a relatively short lifetime. *Phys. Rev. D*, 64:043515, 2001.
- [19] Masahiro Kawasaki, Kazunori Kohri, and Takeo Moroi. Hadronic decay of late - decaying particles and Big-Bang Nucleosynthesis. *Phys. Lett. B*, 625:7–12, 2005.
- [20] Masahiro Kawasaki, Kazunori Kohri, Takeo Moroi, and Akira Yotsuyanagi. Big-Bang Nucleosynthesis and Gravitino. *Phys. Rev. D*, 78:065011, 2008.
- [21] Afif Omar and Adam Ritz. BBN Constraints on the Hadronic Annihilation of sub-GeV Dark Matter. 10 2025.
- [22] Lucia Angel, Giorgio Arcadi, Matheus M. A. Paixão, and Farinaldo S. Queiroz. Updated BBN Bounds on Hadronic Injection in the Early Universe: The Gravitino Problem. 1 2025.
- [23] Ayres Freitas, Frank Daniel Steffen, Nurhana Tajuddin, and Daniel Wyler. Late Energy Injection and Cosmological Constraints in Axino Dark Matter Scenarios. *Phys. Lett. B*, 682:193–199, 2009.
- [24] Dan Hooper, Farinaldo S. Queiroz, and Nickolay Y. Gnedin. Non-Thermal Dark Matter Mimicking An Additional Neutrino Species In The Early Universe. *Phys. Rev. D*, 85:063513, 2012.
- [25] Erminia Calabrese, Dragan Huterer, Eric V. Linder, Alessandro Melchiorri, and Luca Pagano. Limits on dark radiation, early dark energy, and relativistic degrees of freedom. *Physical Review D*, 83(12), June 2011.
- [26] Celine Boehm, Matthew J. Dolan, and Christopher McCabe. Increasing Neff with particles in thermal equilibrium with neutrinos. *JCAP*, 12:027, 2012.
- [27] Maria Archidiacono, Elena Giusarma, Steen Hannestad, and Olga Mena. Cosmic dark radiation and neutrinos, 2013.
- [28] Cara Giovanetti, Martin Schmaltz, and Neal Weiner. Neutrino-dark sector equilibration and primordial element abundances, 2024.
- [29] A.G. Riess L. Verde, T. Treu. Tensions between the early and the late universe. *Nature Astronomy*, 3:891, 2019.
- [30] Eleonora Di Valentino, Olga Mena, Supriya Pan, Luca Visinelli, Weiqiang Yang, Alessandro Melchiorri, David F Mota, Adam G Riess, and Joseph Silk. In the realm of the hubble tension—a review of solutions*. *Classical and Quantum Gravity*, 38(15):153001, jul 2021.
- [31] Alvaro S. de Jesus, Matheus M. A. Paixao, Deivid R. da Silva, Farinaldo S. Queiroz, and Nelson Pinto-Neto. The hubble tension: Relativistic dark matter production from long-lived particles. *Nuclear Physics B*, 1014(116889), 2025.
- [32] Gary Steigman. Primordial alchemy: From the big bang to the present universe, 2002.
- [33] Ryan J. Cooke, Max Pettini, and Charles C. Steidel. One percent determination of the primordial deuterium abundance*. *The Astrophysical Journal*, 855(2):102, March 2018.
- [34] Sandeep Kumar Acharya and Rishi Khatri. Cmb anisotropy and bbn constraints on pre-recombination decay of dark matter to visible particles. *Journal of Cosmology and Astroparticle Physics*, 2019(12):046–046, December 2019.
- [35] Jozef Bucko, Sambit K. Giri, and Aurel Schneider. Constraining dark matter decay with cosmic microwave background and weak-lensing shear observations. *Astronomy & Astrophysics*, 672:A157, April 2023.
- [36] S. S. da Costa, D. R. da Silva, Á. S. de Jesus, N. Pinto-Neto, and F. S. Queiroz. The h_0 trouble: confronting non-thermal dark matter and phantom cosmology with the cmb, bao, and type ia supernovae data. *Journal of Cosmology and Astroparticle Physics*, 35, 2024.
- [37] et al. G.B. Zhao. The clustering of galaxies in the sdss-iii baryon oscillation spectroscopic survey: weighing the neu-

- trino mass using the galaxy power spectrum of the cmass sample. *Monthly Notices of the Royal Astronomical Society*, 436:2038–2053, 2013.
- [38] Jailson Alcaniz, Nicolás Bernal, Antonio Masiero, and Farinaldo S. Queiroz. Light dark matter: A common solution to the lithium and H 0 problems. *Phys. Lett. B*, 812:136008, 2021.
- [39] Riccardo Penco. An introduction to effective field theories. *arXiv preprint*, 2020.
- [40] S. Dodelson and F. Schmidt. *Modern cosmology*. Academic press, 2020.
- [41] N. Aghanim and Others. Planck 2018 results. vi. cosmological parameters. *Astron. Astrophys.*, 641, 2021.
- [42] J. S. Alcaniz, J. P. Neto, F. S. Queiroz, D. R. da Silva, and R. Silva. The hubble constant troubled by dark matter in non-standard cosmologies. *Scientific Reports*, 12:20113, 2022.
- [43] Erminia Calabrese, Maria Archidiacono, Alessandro Melchiorri, and Bharat Ratra. The impact of a new median statistics H_0 prior on the evidence for dark radiation. *Phys. Rev. D*, 86:043520, 2012.
- [44] Stephen M. Feeney, Hiranya V. Peiris, and Licia Verde. Is there evidence for additional neutrino species from cosmology? *JCAP*, 04:036, 2013.
- [45] Simony Santos da Costa, Dêivid R. da Silva, Álvaro S. de Jesus, Nelson Pinto-Neto, and Farinaldo S. Queiroz. The H_0 trouble: confronting non-thermal dark matter and phantom cosmology with the CMB, BAO, and Type Ia supernovae data. *JCAP*, 04:035, 2024.
- [46] M. Hobson, G. Efstathiou, and A. Lasenby. *General relativity: an introduction for physicists*. Cambridge University Press, 2006.
- [47] Max Tegmark, Matias Zaldarriaga, and Andrew J. S. Hamilton. Latest cosmological constraints on the densities of hot and cold dark matter. In *4th International Symposium on Sources and Detection of Dark Matter in the Universe (DM 2000)*, pages 128–137, 2 2000.
- [48] Michael Kopp, Constantinos Skordis, Daniel B Thomas, and Stéphanie Ilić. Dark matter equation of state through cosmic history. *Physical Review Letters*, 120(22), 2018.
- [49] N. Aghanim et al. Planck 2018 results. VI. Cosmological parameters. *Astron. Astrophys.*, 641:A6, 2020. [Erratum: *Astron. Astrophys.* 652, C4 (2021)].
- [50] Wendy L. Freedman and Barry F. Madore. Progress in direct measurements of the Hubble constant. *JCAP*, 11:050, 2023.
- [51] Adam G. Riess et al. A Comprehensive Measurement of the Local Value of the Hubble Constant with $1\text{ km s}^{-1}\text{ Mpc}^{-1}$ Uncertainty from the Hubble Space Telescope and the SH0ES Team. *Astrophys. J. Lett.*, 934(1):L7, 2022.
- [52] M. G. Dainotti et al. A New Master Supernovae Ia sample and the investigation of the Hubble tension. *JHEAp*, 48:100405, 2025.
- [53] Yukei S. Murakami, Adam G. Riess, Benjamin E. Stahl, W. D’Arcy Kenworthy, Dahne-More A. Pluck, Antonella Macoreta, Dillon Brout, David O. Jones, Dan M. Scolnic, and Alexei V. Filippenko. Leveraging SN Ia spectroscopic similarity to improve the measurement of H_0 . *JCAP*, 11:046, 2023.
- [54] Javier E. Gonzalez, Marcelo Ferreira, Leorando R. Colaço, Rodrigo F. L. Holanda, and Rafael C. Nunes. Unveiling the Hubble constant through galaxy cluster gas mass fractions. *Phys. Lett. B*, 857:138982, 2024.
- [55] Alain Blanchard, Jean-Yves Héloret, Stéphanie Ilić, Brahim Lamine, and Isaac Tutusaus. Λ CDM is alive and well. *Open J. Astrophys.*, 7:117170, 2024.
- [56] Leandros Perivolaropoulos and Foteini Skara. Challenges for Λ CDM: An update. *New Astron. Rev.*, 95:101659, 2022.
- [57] Siyang Li, Adam G. Riess, Gagandeep S. Anand, Dan Scolnic, Yukei S. Murakami, Dillon Brout, and Erik R. Peterson. The Complete Sample of Available SNe Ia Luminosity Calibrations from the TRGB Observed with either HST or JWST. *Astrophys. J.*, 997(1):115, 2026.
- [58] Stefano Casertano et al. The Local Distance Network: a community consensus report on the measurement of the Hubble constant at 1% precision. 10 2025.
- [59] Adam G. Riess and Louise Breuval. The Local Value of H_0 . *IAU Symp.*, 376:15–29, 2022.
- [60] Eleonora Di Valentino, Olga Mena, Supriya Pan, Luca Visinelli, Weiqiang Yang, Alessandro Melchiorri, David F. Mota, Adam G. Riess, and Joseph Silk. In the realm of the Hubble tension—a review of solutions. *Class. Quant. Grav.*, 38(15):153001, 2021.
- [61] A. G. Adame et al. DESI 2024 VI: cosmological constraints from the measurements of baryon acoustic oscillations. *JCAP*, 02:021, 2025.
- [62] Sougata Ganguly, Tae Hyun Jung, and Seokhoon Yun. Consistent N_{eff} fitting in big bang nucleosynthesis analysis. 7 2025.
- [63] Eleonora Di Valentino et al. The CosmoVerse White Paper: Addressing observational tensions in cosmology with systematics and fundamental physics. *Phys. Dark Univ.*, 49:101965, 2025.
- [64] Michael Paul Hobson, George P Efstathiou, and Anthony N Lasenby. *General relativity: an introduction for physicists*. Cambridge University Press, 2006.
- [65] Erich Holtmann, M. Kawasaki, Kazunori Kohri, and Takeo Moroi. Radiative decay of a longlived particle and big bang nucleosynthesis. *Phys. Rev. D*, 60:023506, 1999.
- [66] Masahiro Kawasaki, Kazunori Kohri, and Takeo Moroi. Big-Bang nucleosynthesis and hadronic decay of long-lived massive particles. *Phys. Rev. D*, 71:083502, 2005.
- [67] Kazunori Kohri and Fumihiro Takayama. Big bang nucleosynthesis with long lived charged massive particles. *Phys. Rev. D*, 76:063507, 2007.
- [68] Masahiro Kawasaki, Kazunori Kohri, and Takeo Moroi. Big-Bang Nucleosynthesis with Long-Lived Charged Slepton. *Phys. Lett. B*, 649:436–439, 2007.
- [69] Toshifumi Jittoh, Kazunori Kohri, Masafumi Koike, Joe Sato, Kenichi Sugai, Masato Yamanaka, and Koichi Yazaki. Big-bang nucleosynthesis with a long-lived charged massive particle including ^4He spallation processes. *Phys. Rev. D*, 84:035008, 2011.
- [70] Beth A. Reid, Will J. Percival, Daniel J. Eisenstein, Licia Verde, David N. Spergel, Ramin A. Skibba, Neta A. Bahcall, Tamas Budavari, Joshua A. Frieman, Masataka Fukugita, J. Richard Gott, James E. Gunn, Željko Ivezić, Gillian R. Knapp, Richard G. Kron, Robert H. Lupton, Timothy A. McKay, Avery Meiksin, Robert C. Nichol, Adrian C. Pope, David J. Schlegel, Donald P. Schneider, Chris Stoughton, Michael A. Strauss, Alexander S. Szalay, Max Tegmark, Michael S. Vogeley, David H. Weinberg, Donald G. York, and Idit Zehavi. Cosmological constraints from the clustering of the sloan digital sky survey dr7 luminous red galaxies. *Monthly Notices of the Royal Astronomical Society*, March 2010.
- [71] Gong-Bo Zhao, Shun Saito, Will J. Percival, Ashley J. Ross, Francesco Montesano, Matteo Viel, Donald P. Schneider, Marc Manera, Jordi Miralda-Escudé, Nathalie Palanque-Delabrouille, Nicholas P. Ross, Lado Samushia, Ariel G. Sánchez, Molly E. C. Swanson, Daniel Thomas, Rita Tojeiro, Christophe Yèche, and Donald G. York. The clustering of galaxies in the sdss-iii baryon oscillation spectroscopic survey: weighing the neutrino mass using the galaxy power spectrum of the cmass sample. *Monthly Notices of the Royal Astronomical*

Society, 436(3):2038–2053, October 2013.

- [72] Jailson S. Alcaniz, Jacinto P. Neto, Farinaldo S. Queiroz, Deivid R. da Silva, and Raimundo Silva. The Hubble constant troubled by dark matter in non-standard cosmologies. *Sci. Rep.*, 12(1):20113, 2022. [Erratum: *Sci.Rep.* 13, 209 (2023)].
- [73] Alvaro S. de Jesus, Nelson Pinto-Neto, Farinaldo S. Queiroz, Joseph Silk, and Dêivid R. da Silva. The hubble rate trouble: an effective field theory of dark matter. *The European Physical Journal C*, 83(3), 2023.